Bio-hybrid organic semiconductor devices as a platform for the study of biological materials and biosensors

Thomas M. Brown, Janardan Dagar, Manuela Scarselli, Maurizio De Crescenzi, *Shashank Priya*

CHOSE, Centre for Hybrid and Organic Solar Energy, Dept. Electronic Engineering, University of Rome Tor Vergata

Materials Research Institute, Penn State, University Park, PA.

AFRL Work on DNA incorporation in organic electronics

- **DNA Electron Injection Interlayers for Polymer Light-Emitting Diodes**

Peter Zalar, Daniel Kamkar, Rajesh Naik, Fahima Ouchen, James G. Grote,Guillermo C. Bazan, and Thuc-Quyen Nguyen

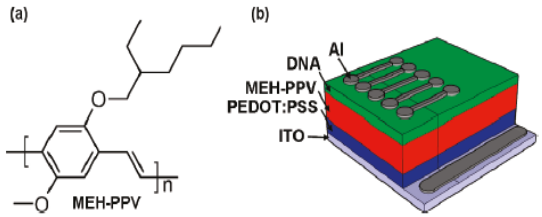

Figure 1. (a) Molecular structure of MEH-PPV. (b) PLED test structure incorporating a DNA interlayer between the Al cathode and the electroluminescent MEH-PPV layer.

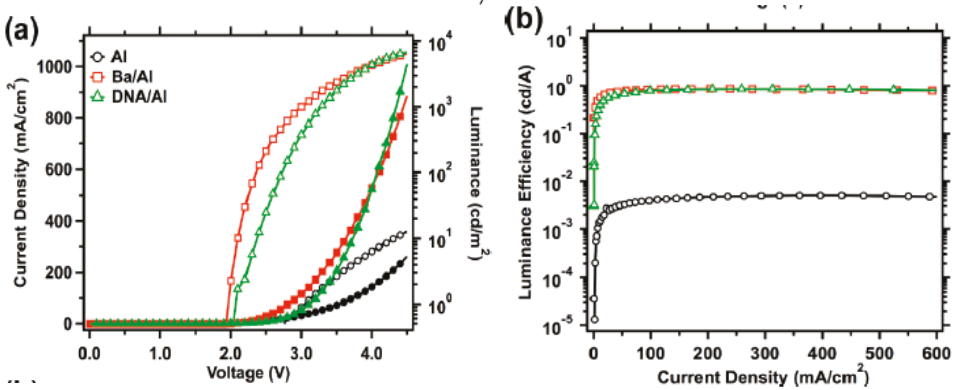

Figure 2. (a) $J-V$ (closed symbols) and $L-V$ (open symbols) plots and (b) luminance efficiency characteristics of PLEDs with the following device structures: ITO/PEDOT:PSS/MEH-PPV/Ba/Al (red squares), ITO/PEDOT:PSS/MEH-PPV/DNA/Al (green triangles), and ITO/PEDOT:PSS/MEH-PPV/Al (black circles).

- **Enhancement of the Photoresponse in Organic Field-Effect Transistors by Incorporating Thin DNA Layers**

Yuan Zhang, Mingfeng Wang, Samuel D. Collins, Huiqiong Zhou, Hung Phan,Christopher Proctor, Alexander Mikhailovsky, Fred Wudl, and Thuc-Quyen Nguyen

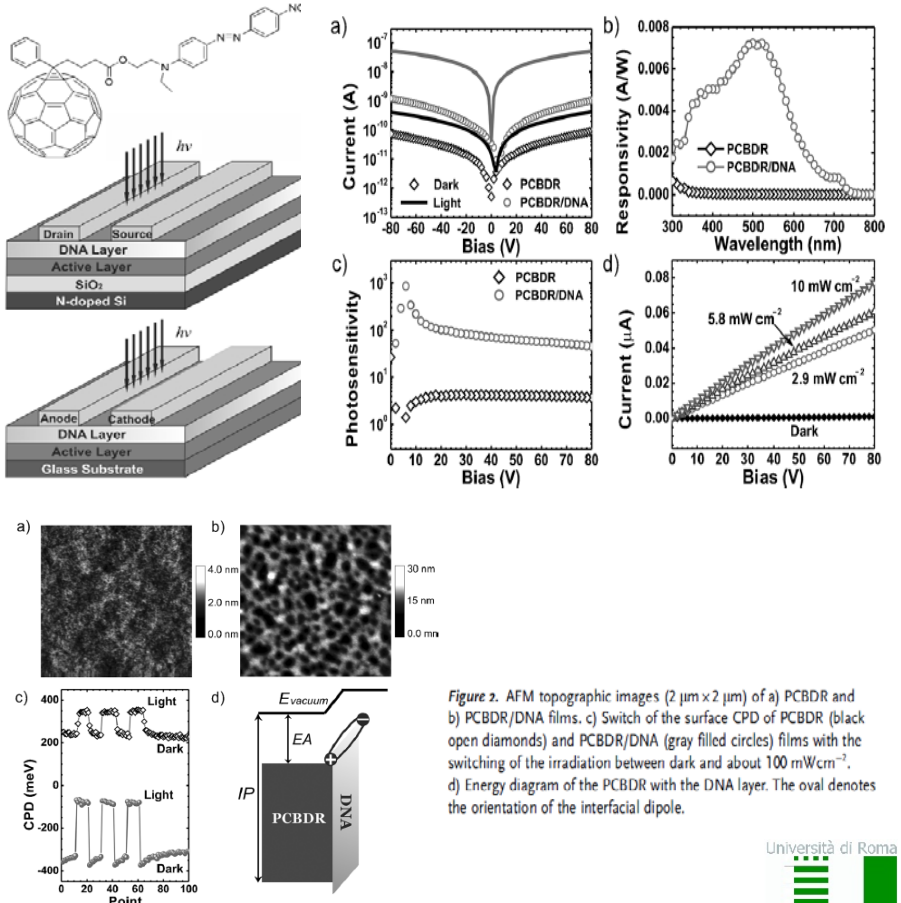

Figure 2. AFM topographic images (2 μm × 2 μm) of a) PCBDR and b) PCBDR/DNA films. c) Switch of the surface CPD of PCBDR (black open diamonds) and PCBDR/DNA (gray filled circles) films with the switching of the irradiation between dark and about 100 mW/cm^{-2}. d) Energy diagram of the PCBDR with the DNA layer. The oval denotes the orientation of the interfacial dipole.

CHOSE

PennState

Università di Roma Tor Vergata

Why combine Solar Cell structure with DNA?

- Controlled photon source provides the ability to model the electron transport through DNA
- Non-contact method for studying the electronic transport
- Modifying the absorber and electrode layers will provide modulation of photo carrier density and thereby provide probe for understanding the role of DNA in electrical signaling

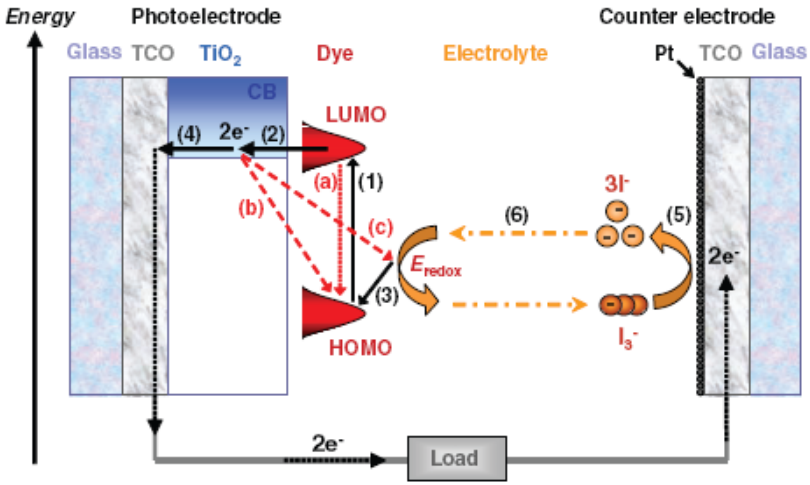

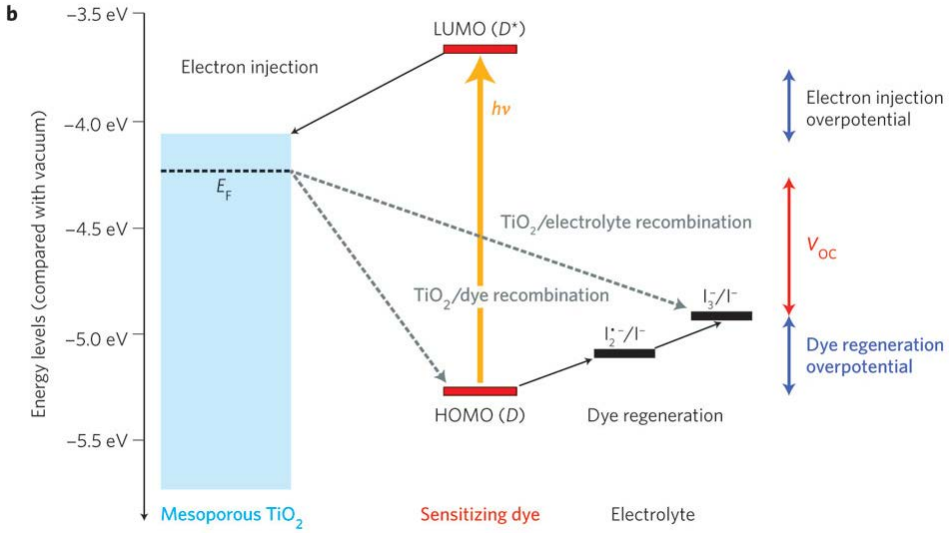

- 1.$S+hv \rightarrow S^*$
- 2. $S^* \rightarrow S^+ + e^-$ (CB)
- 3.e^-(CB) $\rightarrow e^-$ (BC)
- 4.$3I^- + 2S^+ \rightarrow I_3^- + S^*$
- 5. $I_3^- + 2e^- \rightarrow 3I^-$
- 6. $2e^-$(CB) + $I_3^- \rightarrow 3I^-$

CHOSE PennState Università di Roma Tor Vergata

Background of DSSC

❑ How it differs from p-n junction

Dye sensitized solar cell

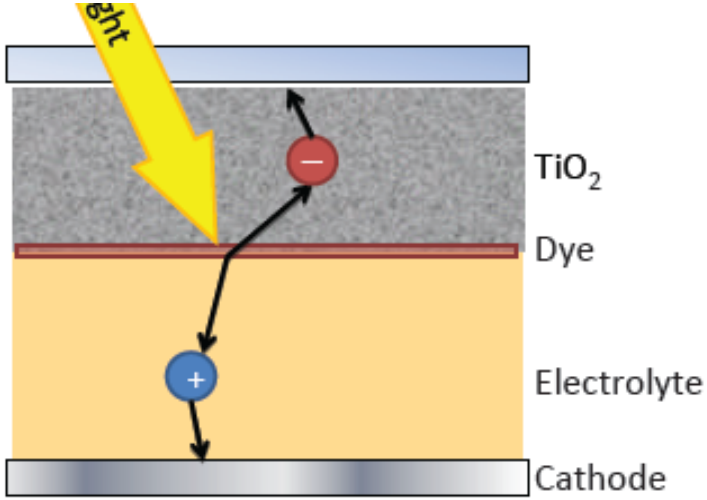

- Light absorption and charge transport are decoupled
- Relaxed constraints on individual components (each can be separately tuned)
- Only monolayer of dye on TiO2

p-n junction Solar cell

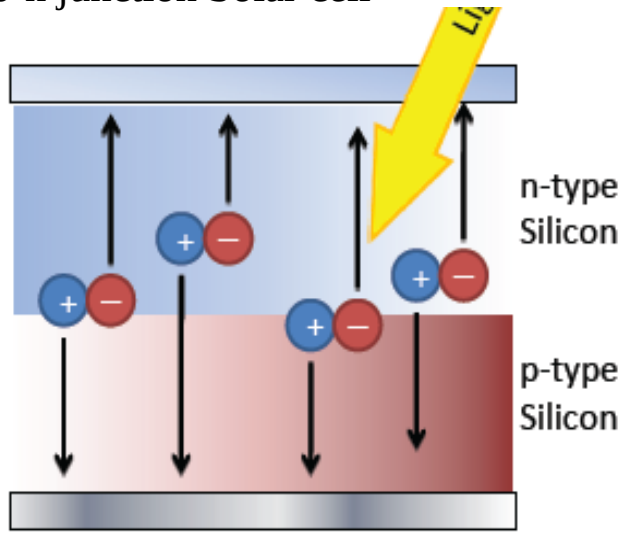

- Charge carriers (excited electrons) are produced throughout the semiconductor
- Semiconductor considerations:
  Precise doping
  High purity
  High crystallinity

Layers of DSSC

❑ Research Field

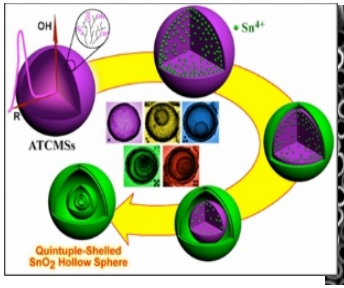

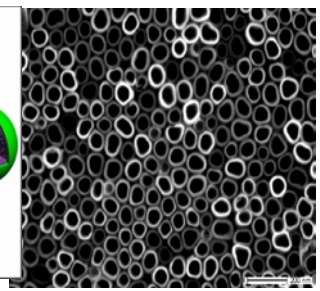

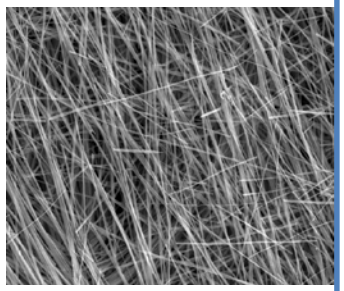

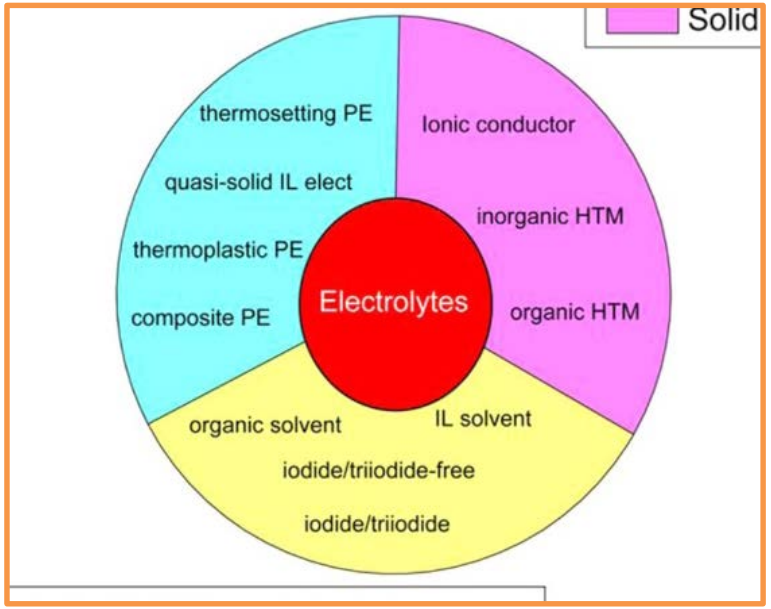

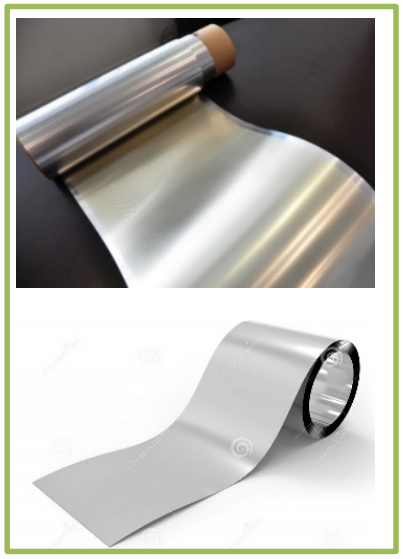

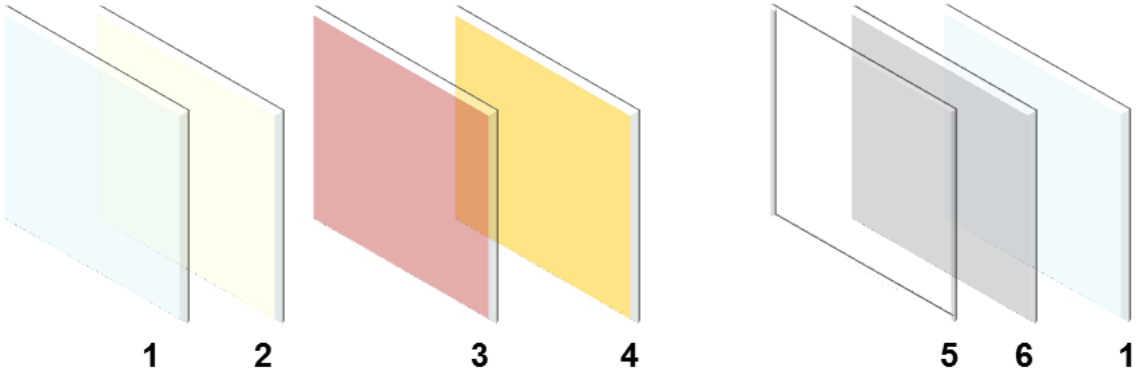

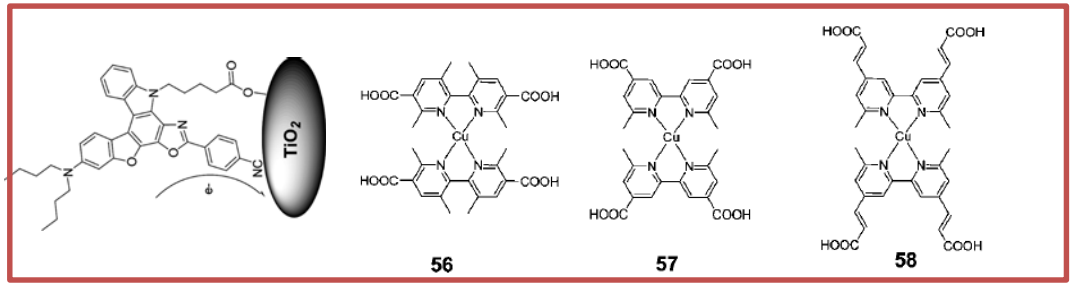

1) Conductive Substrate
2) Titanium Dioxide Nanoparticles
3) Ruthenium Dye
4) Electrolyte
5) Sealing Gasket
6) Platinum Catalyst

VirginiaTech
Invent the Future

Dye Sensitizer

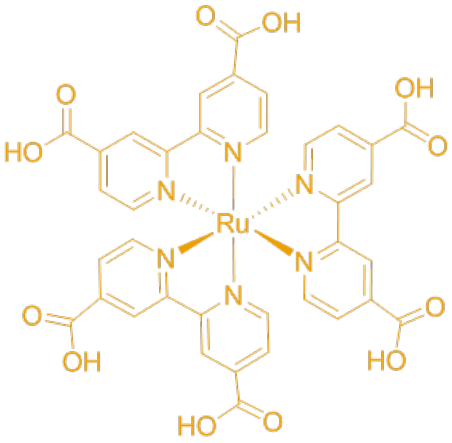

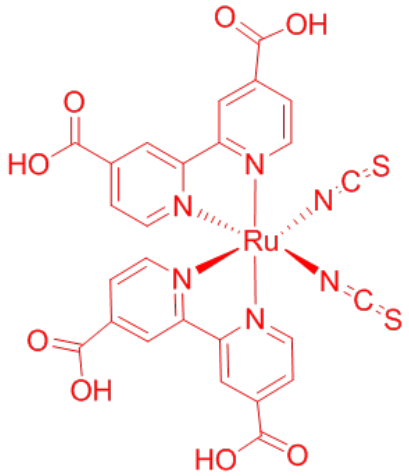

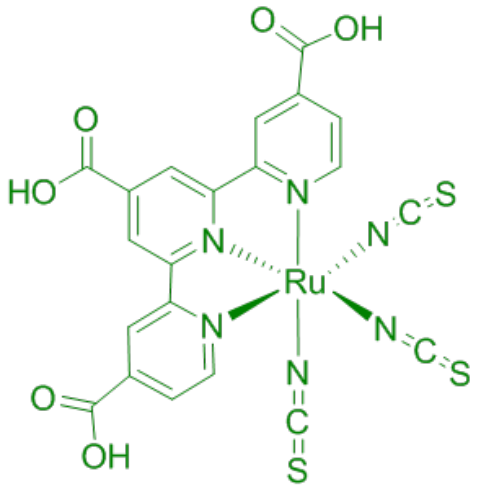

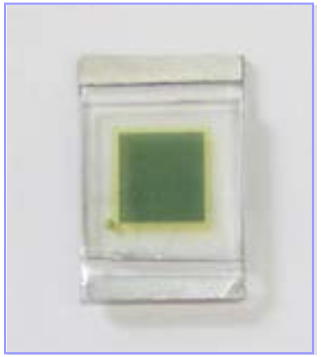

Electrolyte

Requirements

✓ $TiO_2|S+ + 3/2\ I^- \rightarrow TiO_2|S + 1/2\ I_3^-$

- Redox potential
- Self reversible
- Fast diffusion
- No adsorption of light

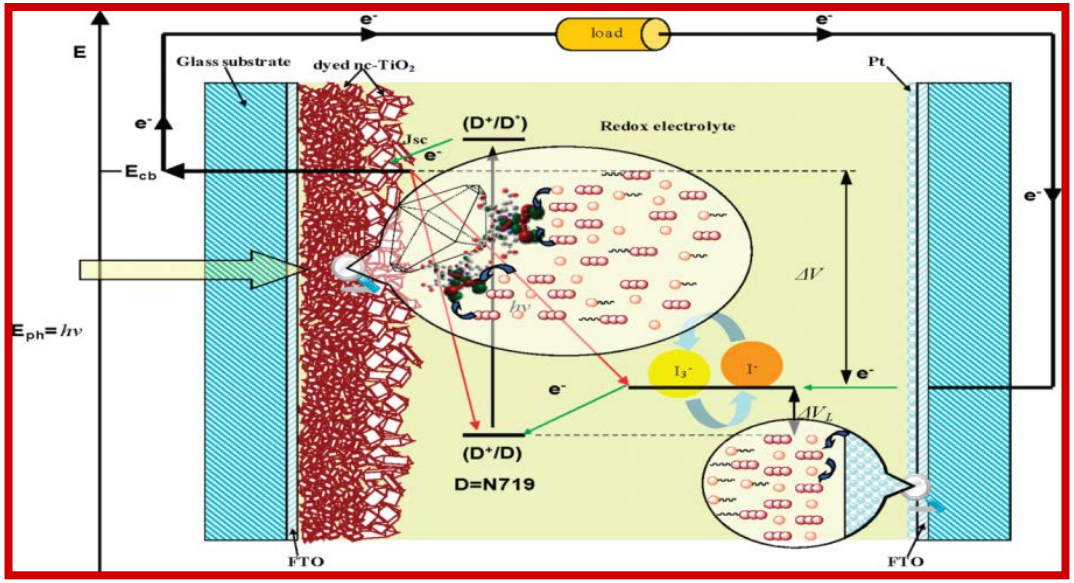

- ◆ Liquid Electrolyte
  - Organic solvent electrolyte
  - Ionic liquid electrolyte
- ◆ Quasi-Solid State Electrolyte
  - Gel polymer electrolyte
- ◆ Solid Electrolyte
  - Polymer electrolyte
  - P-type semiconductors
  - Hole transport materials

Electrolyte

❑ Polymer Electrolyte

Polymer electrolytes stand out because of their excellent properties such as : easy fabrication, low cost and good stability

➢ Gel electrolyte

Lithium cations are dissociated by the organic solvent and are transported through the free volume or micropore of the polymer matrix and the liquid electrolyte

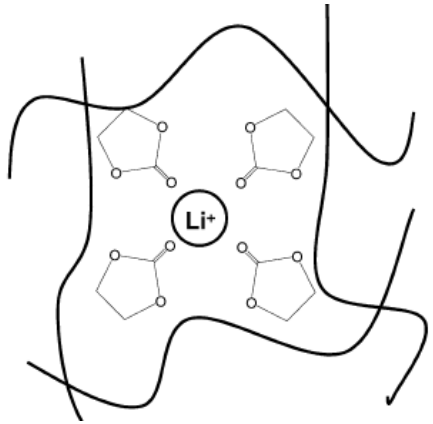

➢ Solid polymer electrolyte

Lithium cations are dissociated by the polymer matrix and transported through Lewis acid–base interactions in the free volume of the matrix, assisted by polymer segmental motion.

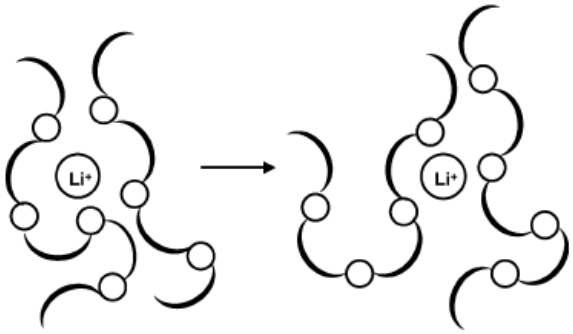

Notice the cell fabrication process – Offers ability to control the charge transport through DNA

❖ Perovskite Solar Cell Structure

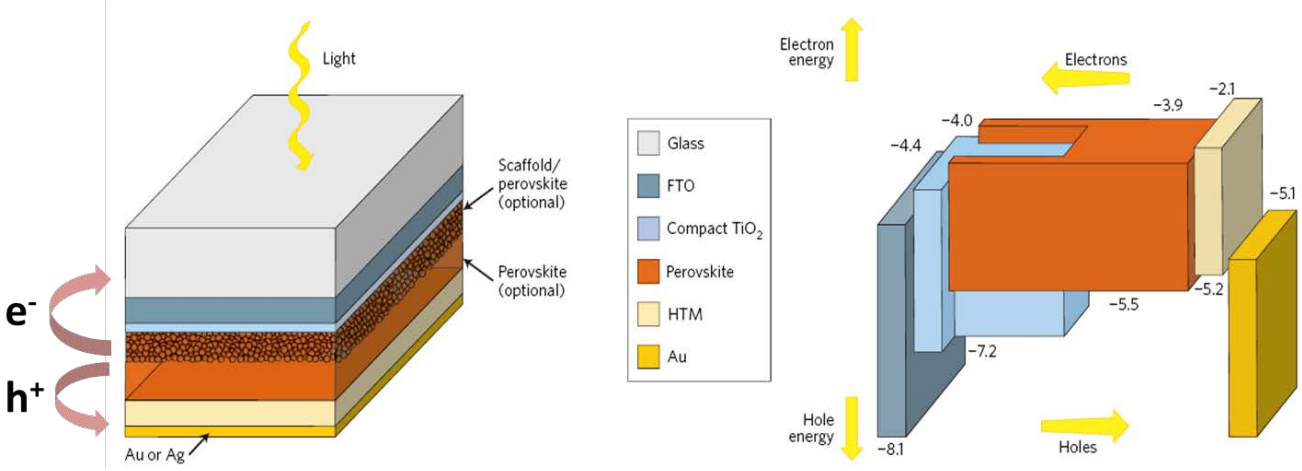

❖ Perovskite Solar Cell Fabrication

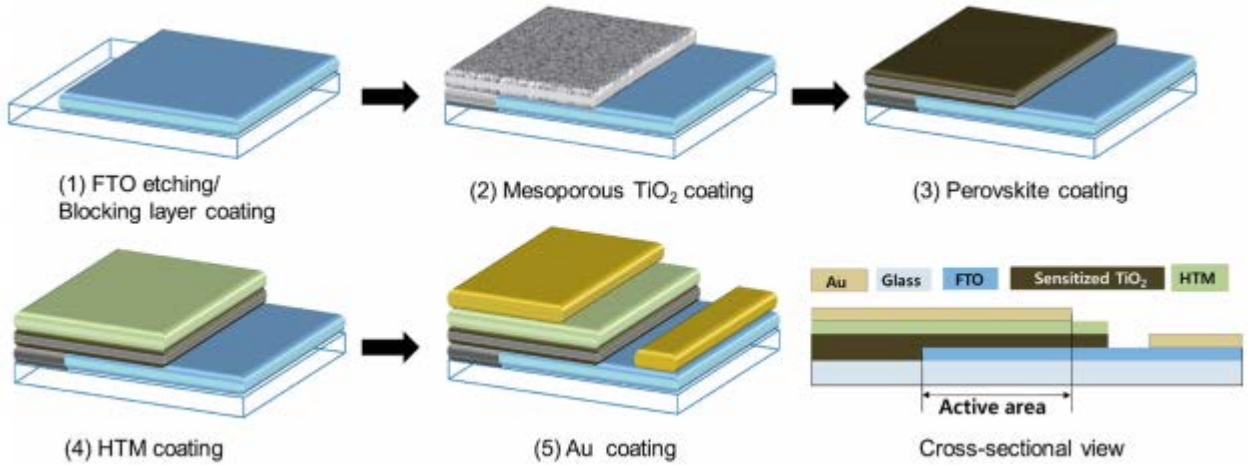

Green, M. A, et al., *Nat. Photon*, **2014**, 8, 506

Solar cells incorporating DNA EELs

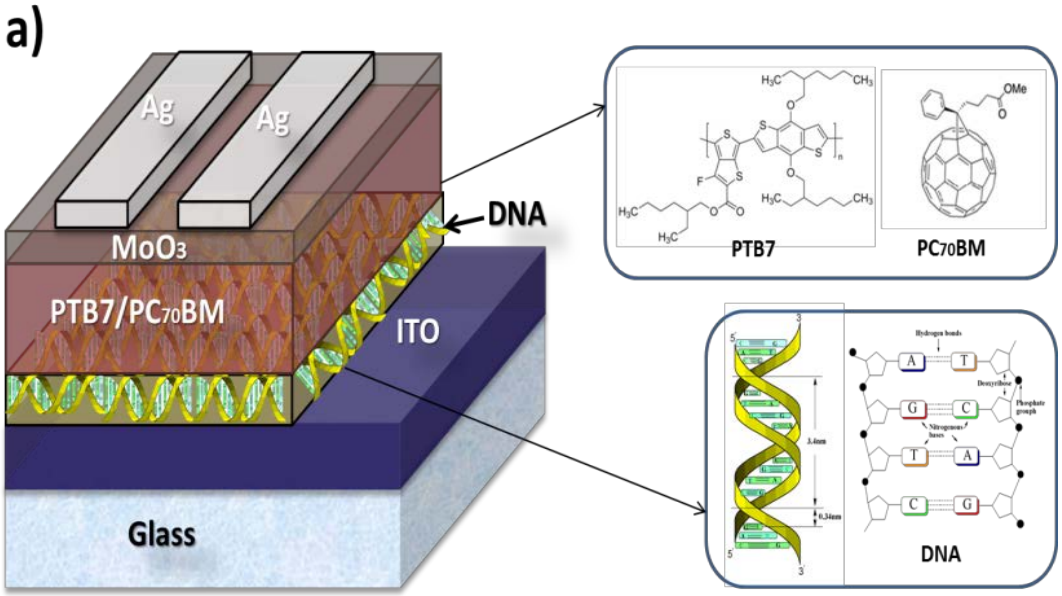

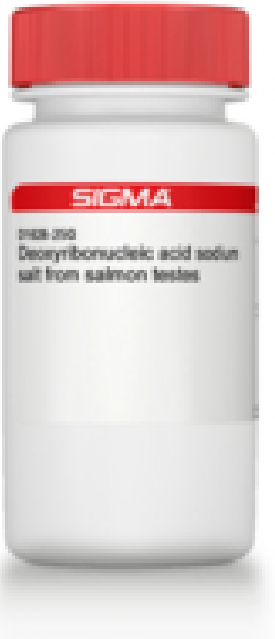

- **DNA (Deoxyribonucleic acid sodium salt from salmon, molecular mass of 1.3 × 10^6 Da (~2,000 bp)).**
- **DNA spin-coated from a water:methanol solution**
- **DNA thickness between 1-10nm**
- **<u>First Time «natural» DNA successfully incorprated in a solar cell</u>**

Device characteristics Solar cells incorporating DNA EELs

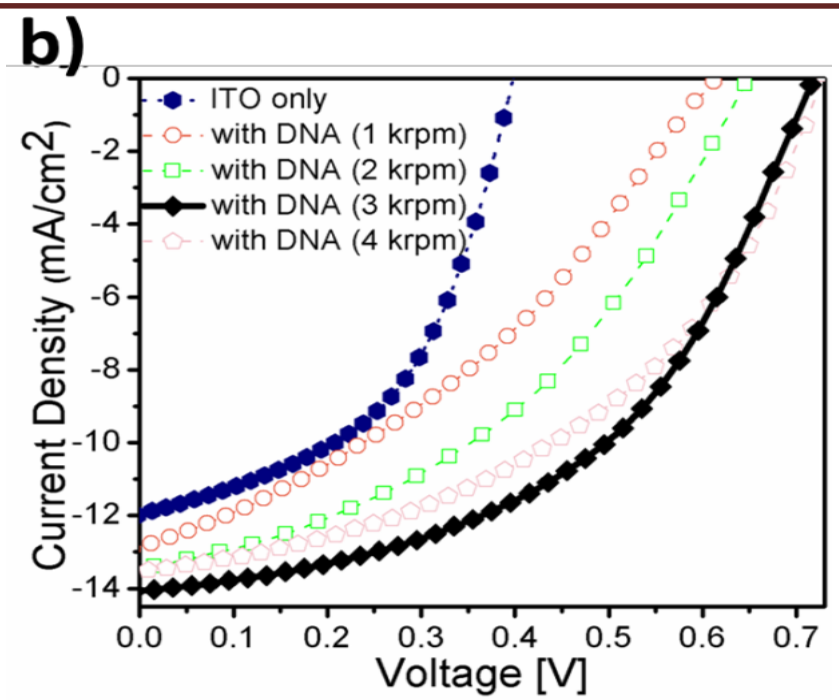

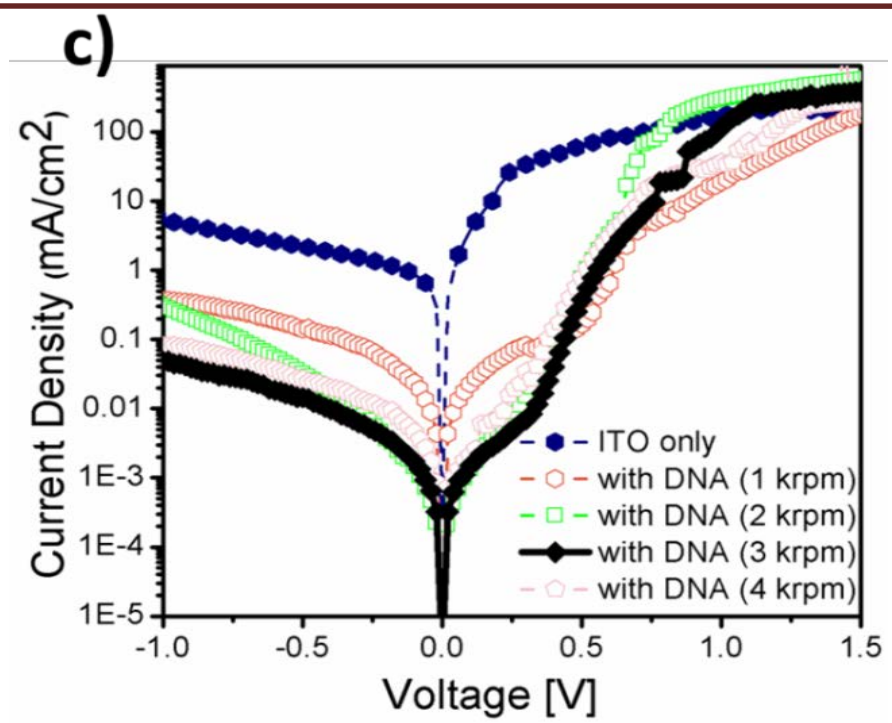

- **Insertion of DNA between photoactive layer and ITO leads to remarkable improvement in :**
  - **<u>PV parameters (Fig. b): Efficiency from 2% to 5%</u>**
  - **<u>On/off ratios in the dark (Fig. c) by a factor of 125</u>**
- **Thickness optimization for best performance**

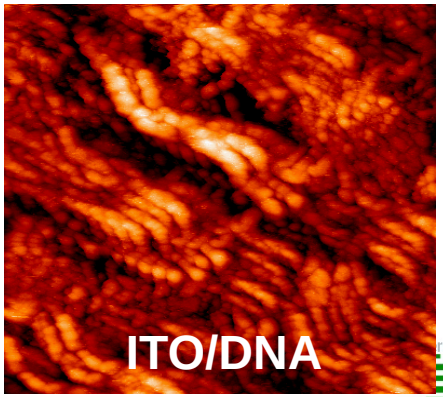

CHOSE PennState

Solar Cells Incorporating DNA Nanolayers, J. Dagar,..Brown, ACS Energy Lett. 2016

Tor Vergata

STM images and energy level diagram

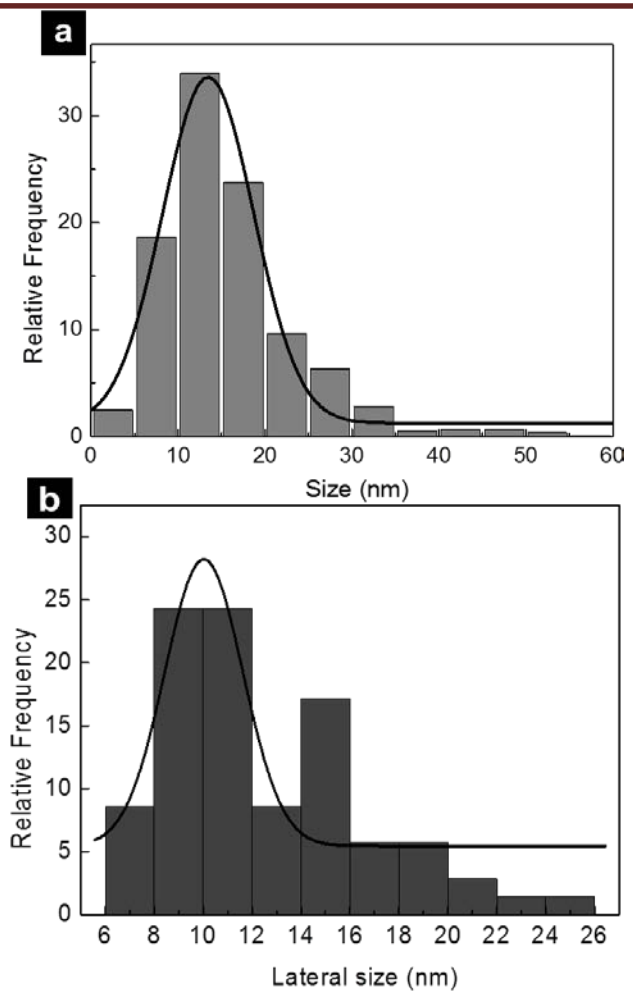

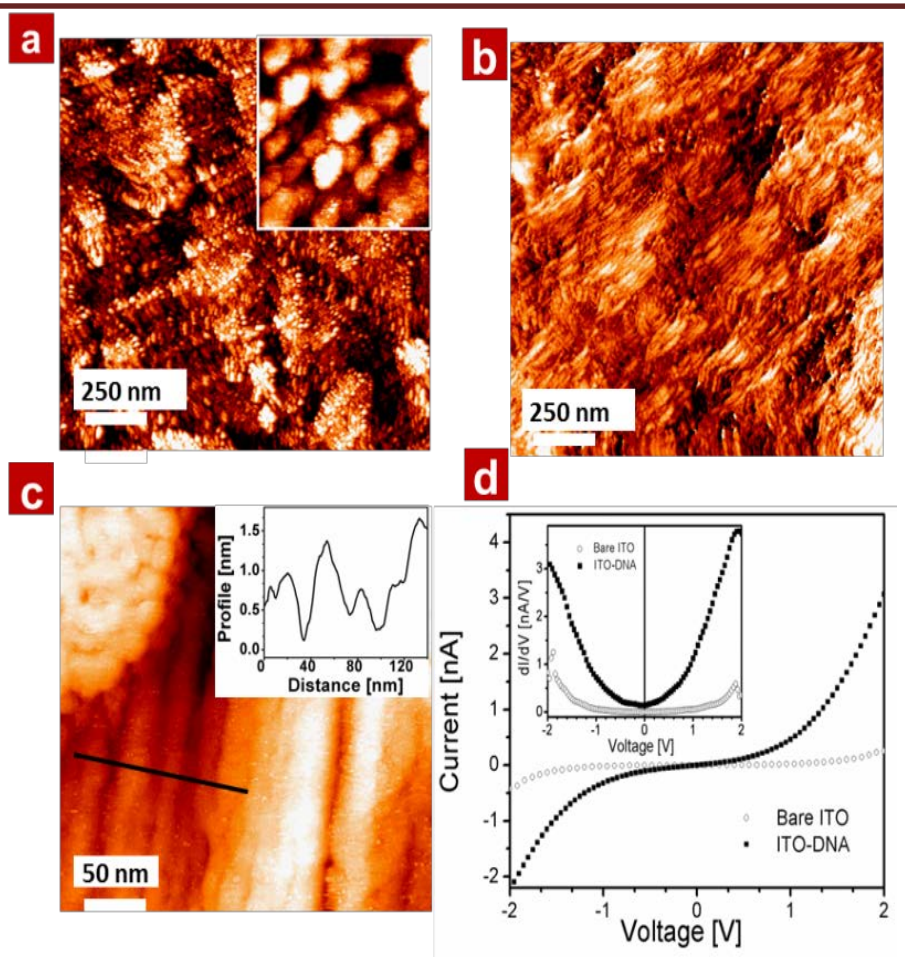

(a) Cluster size distribution from ITO bare surface with Gaussian fit: 13 ± 0.3 nm and (b) Lateral size distribution of DNA bundles deposited on ITO surface with Gaussian fit: 10.02 ± 0.43 nm

STM of the ITO and ITO/DNA

3D Aerosol Printing

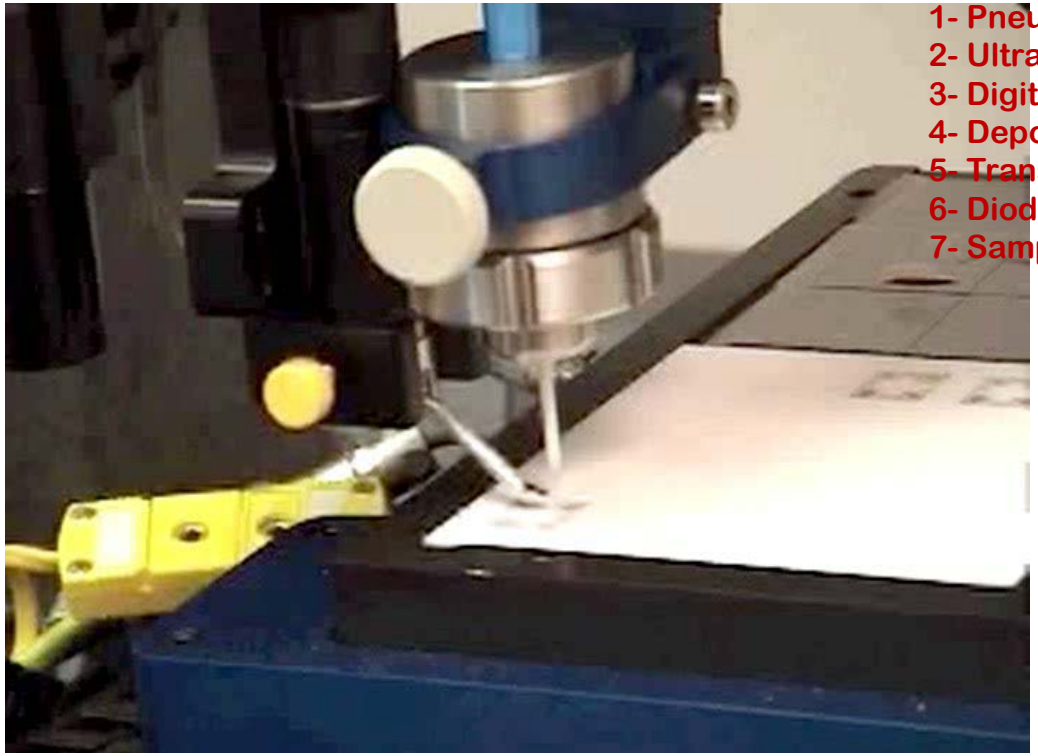

1- Pneumatic atomizer
2- Ultrasonic atomizer
3- Digital cameras
4- Deposition module
5- Translation stage
6- Diode laser module
7- Sample Platen (12x12in)

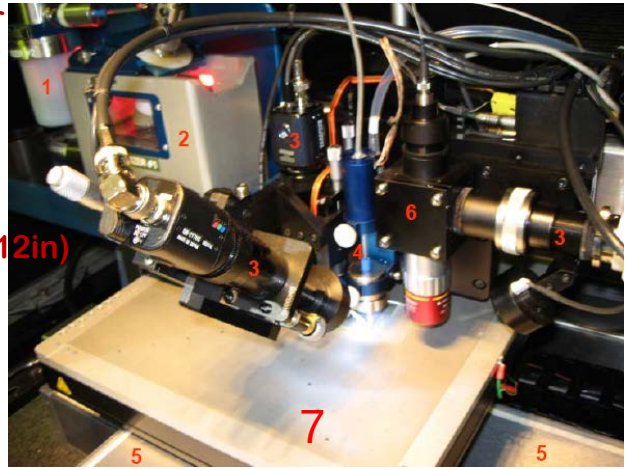

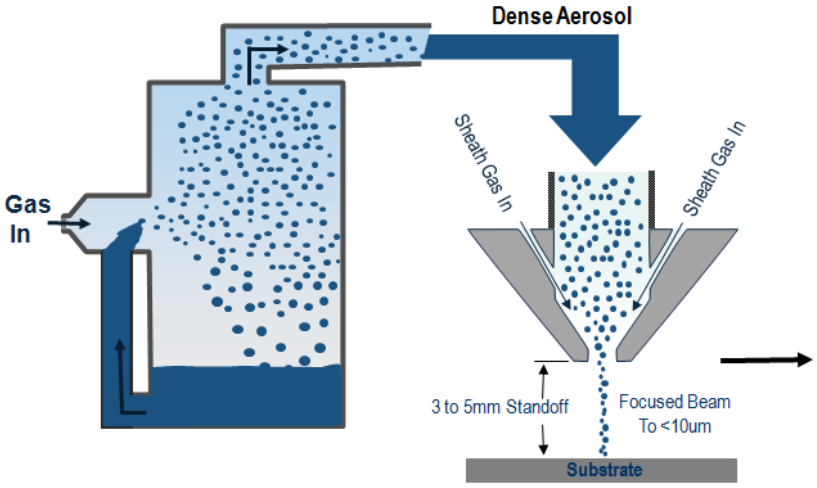

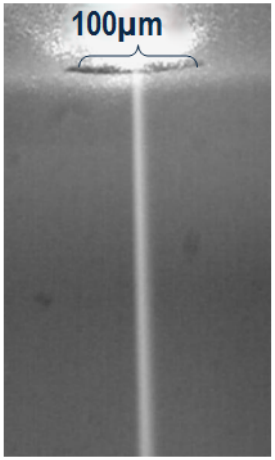

Focused Material Beam

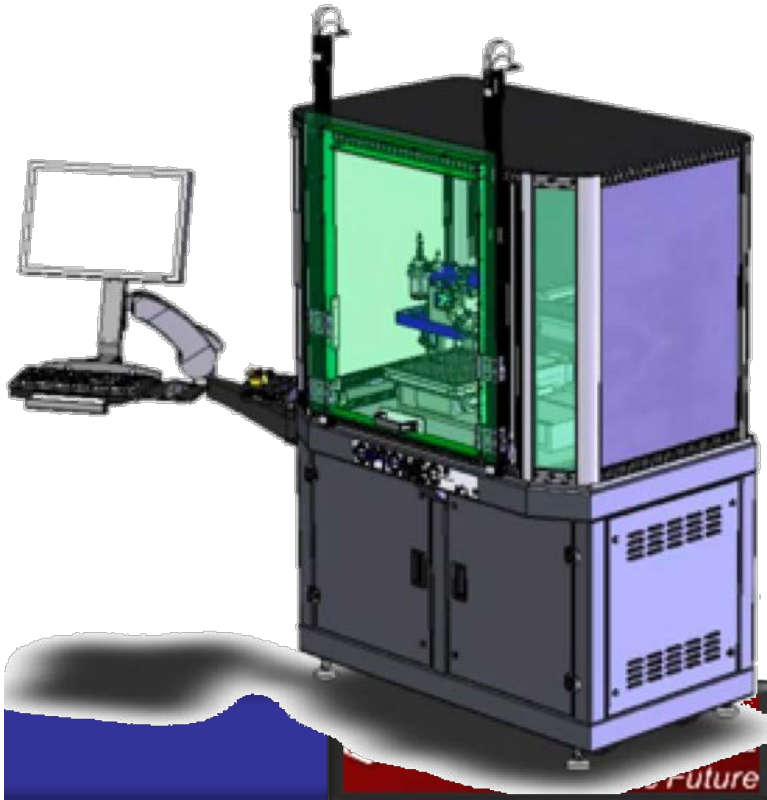

Laser effect

Laser selection - penetration depth

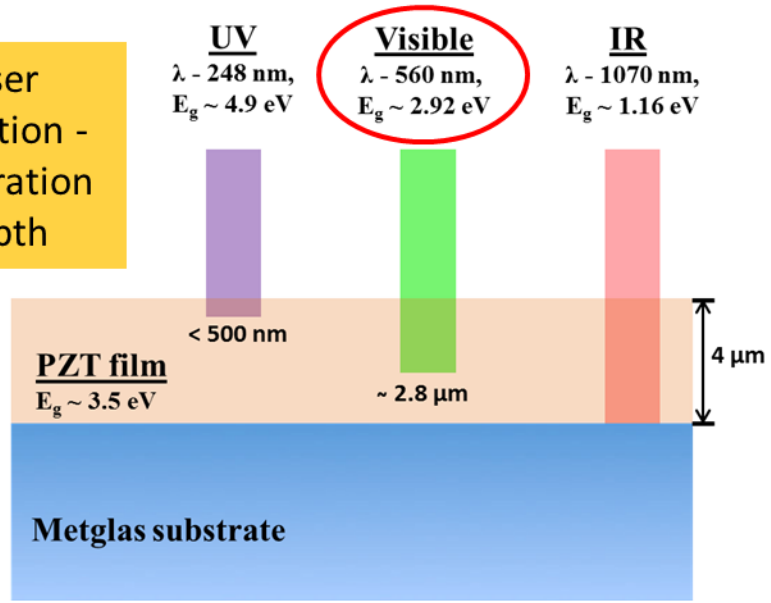

Laser absorption – due to band gap changes in disordered structure

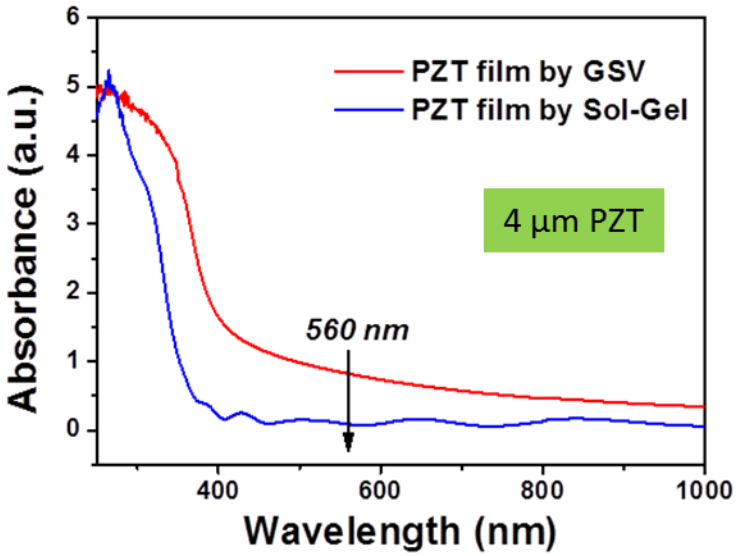

Laser heat localization – limited diffusion – low thermal conductivity of PZT by GSV

- Penetration depth, d = 2.8 µm $\{\frac{1}{d} = \alpha = -\frac{1}{t_{PZT}} ln(\frac{T}{1-R})\}$
- Diffusion length, x = 1550 µm $\{x = \sqrt{2D\tau} = \sqrt{2\left(\frac{k}{\rho C_p}\right)\tau}\}$
- Thermal conductivity, $k = (\frac{1}{3})C_p v L$
- ✓ GSV film – amorphous (disorder) + nanocrystalline (more # GBs)

High speed collisions - fracturing

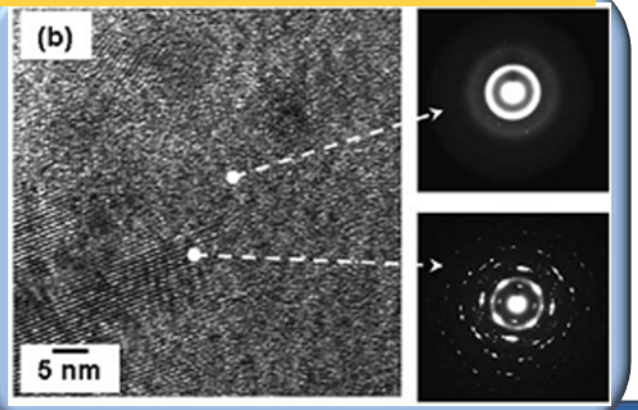

Choi, JJAP, 2007

Microstructural change due to laser annealing

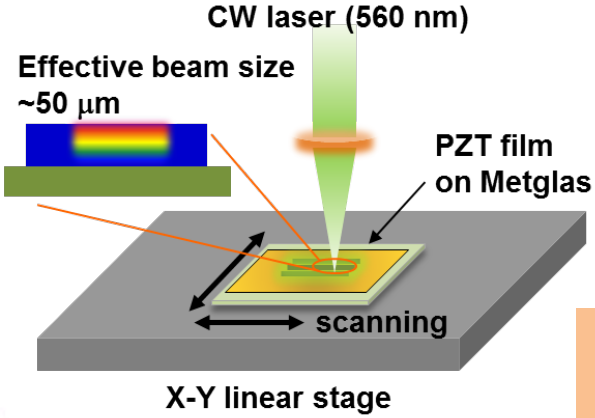

LA regions

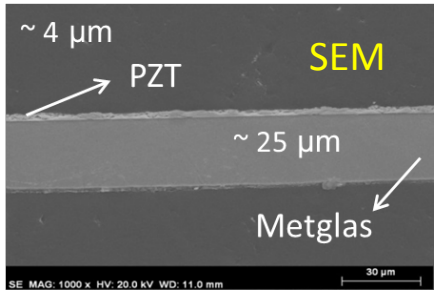

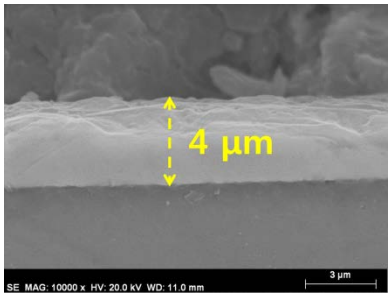

- ✓ Highly dense & well-bonded PZT film (4 μm) on Metglas (25 μm)
- ✓ Annealing – laser power (220 mW), scan speed (0.05 mm/s)

XRD

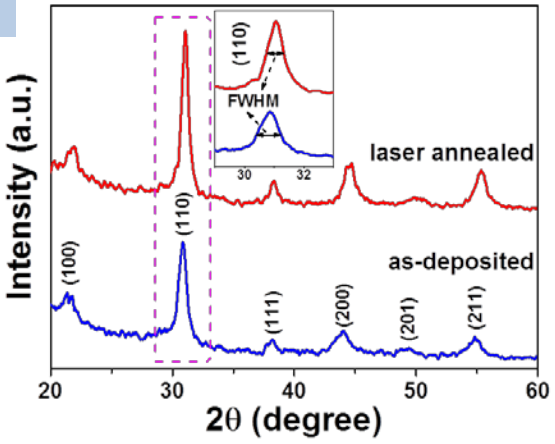

TEM – microstructural change

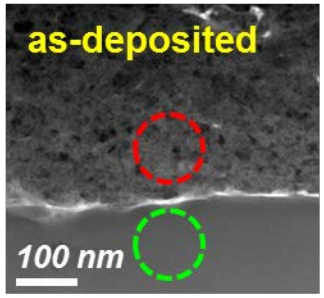

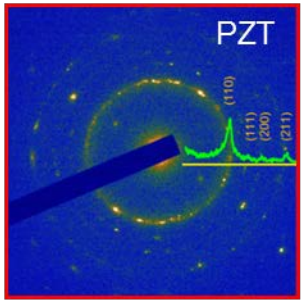

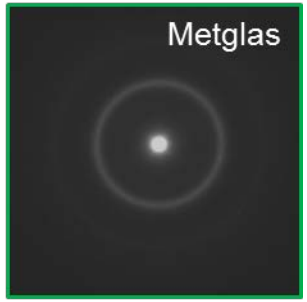

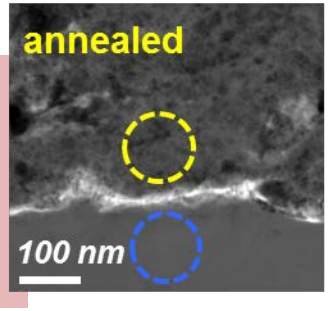

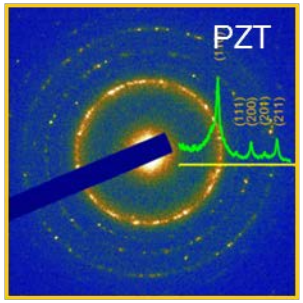

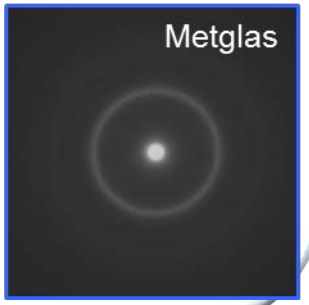

- ✓ as-dep PZT → amorphous & crystalline
- ✓ annealed PZT – crystallinity & grain size ↑
- ✓ no change in amorphous Metglas structure

In-situ microstructure analysis

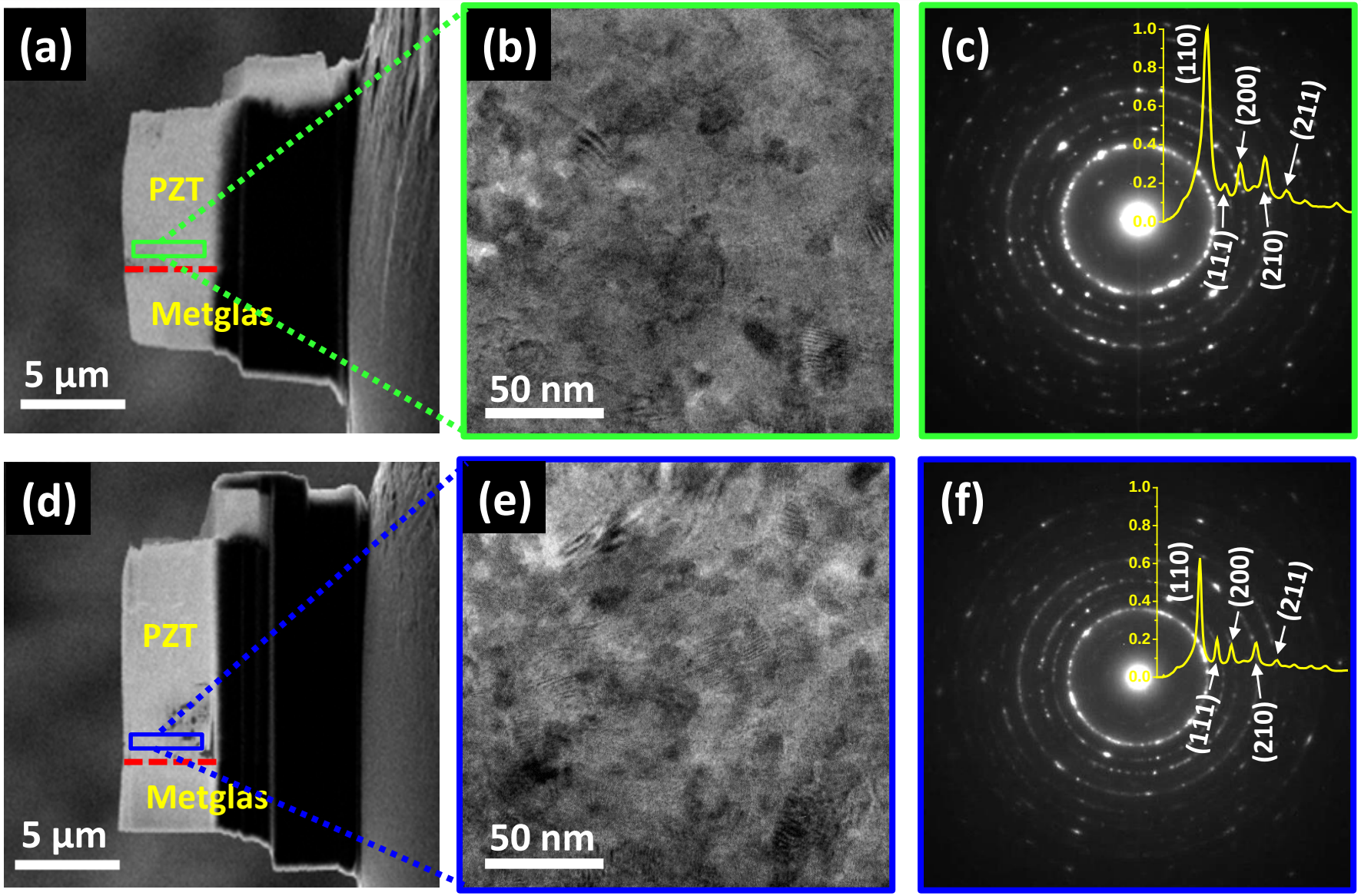

Summary

Non-contact characterization method for quantifying the electronic transport in biological materials.

Ability to design samples through nanoprinting and laser annealing as needed to understand the function in realistic environment.

Provides excellent capability to apply the external controls – magnetic field, thermal field and strain field.